ORGANOMETALLICS

ARTICLE

pubs.acs.org/Organometallics

Activation of an Unstrained C(sp^2)−C(sp^2) Single Bond Using Chelate-Bisphosphinite Rhodium(I) Complexes

Andreas Obenhuber and Klaus Ruhland*

Lehrstuhl für Chemische Physik und Materialwissenschaften, Institut für Physik, Universität Augsburg, Universitätsstrasse 1, D-86159 Augsburg, Germany, and Lehrstuhl für Anorganische Chemie, Department Chemie, Technische Universität München, Lichtenbergstrasse 4, D-85747 Garching bei München, Germany

Supporting Information

ABSTRACT: The reaction of $[Rh(coe)_2Cl]_2$ with the ligands P(^{i}Pr)$_2$-O-Ph^{pX}-CO-Ph^{pX}-O-P(^{i}Pr)$_2$ (**L1** X = H and **L2** X = OMe) containing a benzophenone moiety resulted in the quantitative oxidative addition of the PhC−CO single bond under very mild conditions (193 K, **2a**/**b**). For **L2** the mechanism and the kinetics of the oxidative addition were investigated. Only complex **2a** (X-ray crystal structure included) shows an exchange of the metal-bonded carbon moieties via migratory extrusion/insertion (**3a**) in solution. Thermodynamic parameters for this process were determined (for **3a** → **2a** ΔH° = 9.3 ± 0.5 kJ/mol, ΔS° = 53.8 ± 1.8 J/(K mol)). The further fate, in particular the reductive elimination, of **2a**/**b** was investigated and compared to the behavior of Ir. The reaction of **2a**/**b** with several Lewis bases such as CO, ^{13}CO, *tert*-butyl isonitrile, pyridine, acetonitrile, and ^{15}N-acetonitrile was investigated. DFT calculations for the most important steps were performed.

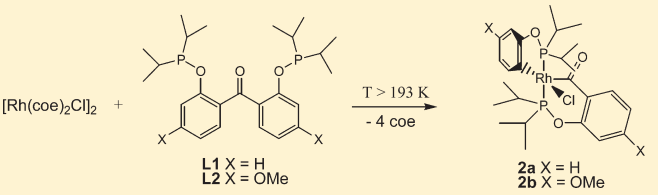

INTRODUCTION

C−C single bond activation using transition metal complexes has lost neither its attraction nor its challenging character in current organometallic chemistry.[1] Several driving forces have been applied: relief of ring strain,[2] aromatization,[3] chelating or coordinating assistance, and/or coupling to energy releasing steps (e.g., liberation of CH_4).[4,5] Inter- and intramolecular activation of $C_{carbonyl}-C_\alpha$ bonds, which are considered slightly weaker compared to other C−C single bonds,[6] has also been demonstrated. Rhodium(I) precursors were very promising as a metal source. Ito, Murakami, et al. used stoichiometric amounts of $(PPh_3)_3RhCl$ for the decarbonylation (via $C_{carbonyl}-C_\alpha$ bond cleavage as proposed) of cyclobutanones, cyclopentanones, and cyclododecanone.[4f,g] Brookhart et al. applied bulky cyclopentadienylrhodium ethylene complexes for the decarbonylation of benzophenones, acetophenones, and α,β-unsaturated ketones. A precoordination of the substrate as η^4-enone was found.[4h] Similar Rh(I) complexes were used by Jones et al. for the C(sp^2)−C(sp^2) single bond cleavage in the strained biphenylene.[4i,j] Rh(I) complexes have also been used to activate $C_{carbonyl}-C_\alpha$ bonds in special substrates.[4s−u] The catalytic decarbonylation of alkyl phenyl ketones bearing oxazoline or pyridine groups on the phenyl ring by $Ru_3(CO)_{12}$ was also reported.[4k] Quite forcing reaction conditions were necessary in all these systems (temperatures higher than 373 K). Suggs et al. applied 8-quinolinyl acetylenic/alkyl or aryl ketones to $RhCl(PPh_3)_3/[(C_2H_4)_2RhCl]_2$, resulting in the formation of acylrhodium(III) complexes at room temperature.[4l−p] A variant of this system uses 2-amino-3-picolylimines.[4q,r] Milstein et al. studied the cleavage of C(sp^2)−C(sp^3) bonds in their PCX (X = P, N, O) pincer-type system,[5] demonstrating the possibility of selective C−C activation (vs C−H) under mild conditions.[5b,g,o]

We extended our studies on nonstrained C(sp^2)−C(sp^2) single bond activation using bisphosphinite ligands further to group 9 transition metals.[7] Herein we report the chelate-assisted insertion of Rh(I) into a benzophenone moiety under remarkably mild conditions. We compare this behavior with our findings about the analogous chemistry of Ir published before.[8]

RESULTS AND DISCUSSION

Activation of the C−C Single Bond. The reaction between $[Rh(coe)_2Cl]_2$ and the ligands **L1** and **L2** (Scheme 1) results in the last instance in the quantitative oxidative addition of the PhC—CO bond even at 193 K in toluene (Figure 1: sharp doublet of doublets at 157 and 180 ppm).

In the case of **L2** we were able to experimentally go more into detail concerning the complete reaction of $[Rh(coe)_2Cl]_2$ with this ligand.

Figure 1 shows the ^{31}P NMR spectroscopic results for the reaction of **L2** with $[Rh(coe)_2Cl]_2$ at different temperatures from 193 to 303 K. As can be seen from these spectra, even at 193 K an instantaneous and complete coordination of the ligand to the Rh center occurs (two broadened doublets at 170 ppm ($^1J_{PRh}$ = 178 Hz) and 205 ppm ($^1J_{PRh}$ = 217 Hz); the olefinic peaks of the coe in ^{1}H NMR are broadened as well). The value of the $^1J_{PRh}$ coupling constant proves that this complex contains the Rh still

Received: April 8, 2011
Published: July 05, 2011

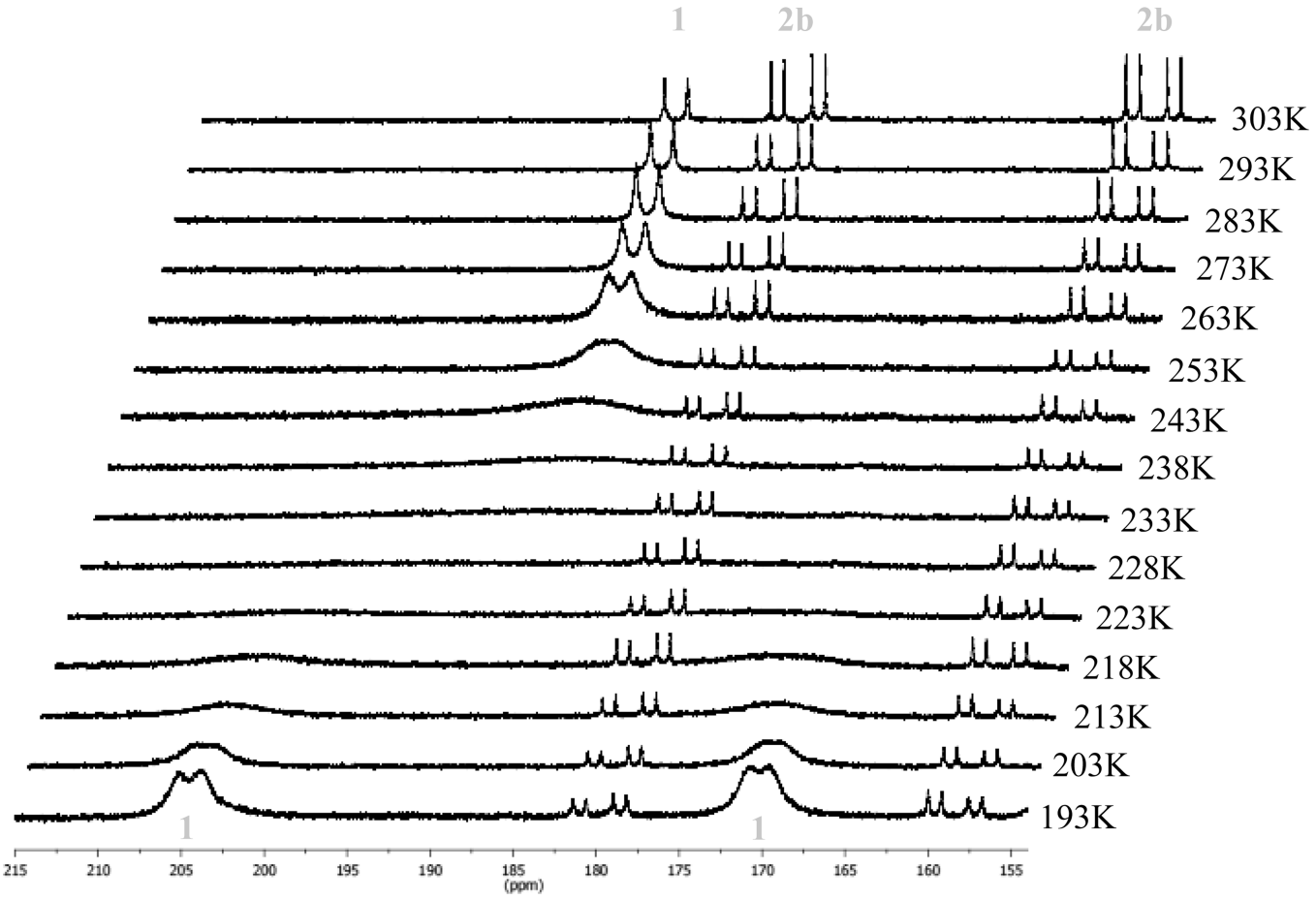

Figure 1. Development of the reaction of 2.1 equiv of **L2** with $[Rh(coe)_2Cl]_2$ in toluene-d_8. $^{31}P\{^1H\}$ NMR spectra were recorded between 193 K (bottom) and 303 K (top).

Scheme 1

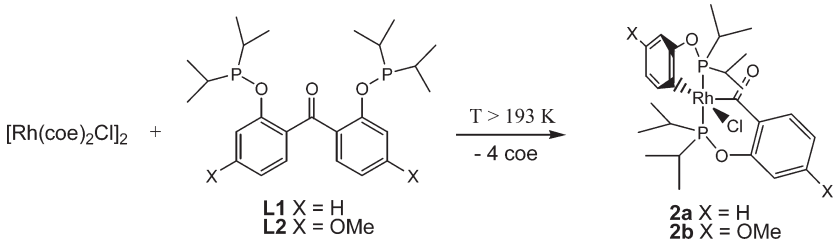

in the oxidation state +I. A $^2J_{PP}$ coupling cannot be resolved. From this finding it can be concluded that the two inequivalent P atoms are in *cis* configuration to each other during the majority of time since in the case of a *trans* configuration the $^2J_{PP}$ coupling should be visible as two doublets of doublets in spite of the broadened peaks. Even at 193 K in the first spectrum the activated complex is already detected in a considerable amount (Figure 1: sharp doublet of doublets at 157 and 180 ppm). At higher temperatures the two broad doublets show coalescence at T_c = 228 K into one sharp doublet ($^1J_{PRh}$ = 229.9 Hz) at the center of gravity of the two starting doublets at 187 ppm. Applying a complete line shape analysis[9] on the dynamic process of Rh(I) complex **1** (Figure 2) leads to the activation parameters $\Delta H^{\#}$ = 40 ± 1 kJ/mol and $\Delta S^{\#}$ = 11 ± 5 J/(mol K). The activation entropy excludes pure associative or dissociative rate-determining steps. The exchange kinetics is concentration-independent (checked at 0.11 and 0.055 mol/L).

If $[Rh(ethene)_2Cl]_2$ is reacted with ligand **L1** or **L2**, only the activation of the C−C single bond is observed (sharp doublet of doublets at 157 and 180 ppm) without preceding dynamic behavior of any other complex. This proves that the process found with $[Rh(coe)_2Cl]_2$ must involve the coe in a decisive role and cannot just be explained by a [**L1**/**2**RhCl] moiety. Addition of excess coe did not slow the dynamic behavior of complex **1** (in accordance with the concentration independence of the exchange) or lead to a resolution of the $^2J_{PP}$ coupling, but it reduced the rate of the following activation step. Addition of 12 equiv of norbornene as an even more strained olefin did not trap

dx.doi.org/10.1021/om200288e |*Organometallics* 2011, 30, 4039–4051

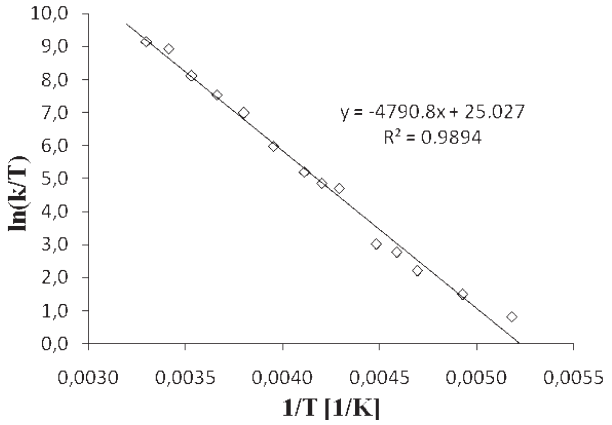

Figure 2. Eyring plot for the exchange in the Rh(I) complex **1**.

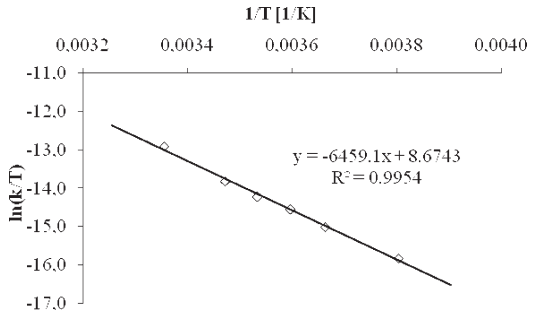

Figure 3. Eyring plot for the first-order evaluation of the C−C single bond activation in **1** using **L2**.

the exchange in the Rh(I) complex **1** either. A trapping does take place with pyridine, resulting in two doublets of doublets ($^2J_{PP}$ = 36.9 Hz, 167 ppm, $^1J_{PRh}$ = 222.45 Hz, 205 ppm, $^1J_{PRh}$ = 201.2 Hz) in the ^{31}P NMR spectrum with resolved $^2J_{PP}$ coupling proving the *cis* configuration of the P atoms. Still the activation of the C−C single bond cannot be stopped even in pure pyridine.

The kinetics of the activation step for **L2** was quantified by integrating the signals in the ^{31}P NMR spectrum for Rh(I) complex **1** and those for the activated compound dependent on time and temperature. This was done in the range between 263 and 298 K (Figure 3, Table 1). The evaluation was performed assuming first-order equations for the kinetic description (c = 0.04 mol[Rh]/L).

From this evaluation the activation parameters $\Delta H^{\#} = 54 \pm 2$ kJ/mol and $\Delta S^{\#} = -125 \pm 7$ J/(K mol) can be extracted. The large negative activation entropy supports an associative rate-determining step for the C−C single bond activation in **L2**, although it does not prove it. No CH activation could be detected by ^{1}H NMR spectroscopy in the range from 20 to −40 ppm throughout the whole C−C single bond activation.

We propose the reaction pattern in Scheme 2 as an explanation for the activation reaction and the dynamic behavior of the Rh(I) complex **1**.

It will be further supported by DFT calculations below.

The dynamic behavior of the Rh(I) complex **1** is explained by an intramolecular exchange of the Cl/coe ligands in **1**. We propose that this process is brought about by a temporary interaction of the CO moiety of the ligand with the metal center. DFT calculations performed by us (B3LYP/LanL2DZ) support

Table 1. Rate Constants (first-order evaluation) for the C−C Single Bond Activation in 1 Using L2 at Variable Temperatures

T [K]	k_{OxAd} [s^{-1}] × 10^4
263	0.35(1)
273	0.83(2)
278	1.34(2)
283	1.88(4)
288	2.87(4)
298	7.41(18)

that the interaction is of O-η^1-manner. The experimentally found concentration independence of the dynamic behavior excludes a coe dissociation/association or a monomer/dimer equilibrium, in accordance with the results of the DFT calculations. No reduced wavenumber for the carbonyl group could be observed during the dynamic behavior, though. The observed wavenumber is the same as in the free ligand.

From complex **1**, coe is dissociated in a non-rate-determining step (activation entropy for C−C-scission negative), leading to a coe-free intermediate from which the rate-determining activation of the C−C single bond takes place with a remarkably low activation barrier. A precoordination of the CO moiety cannot be directly detected or observed. That the ligand architecture in **L1** and **L2** would allow a precoordination of the CO moiety in principle can be proven by applying a ligand that contains a methylene group instead of the oxo. In that case a pure η^2-coordination of the double bond to Rh is observed without any C−C single bond cleavage (compound **2′** in Scheme 3). In the resulting compound the two P atoms couple with each other with $^2J_{PP}$ = 442.5 Hz, proving their *trans* configuration. The two $^1J_{PRh}$ coupling constants are, with 133.7 and 136.6 Hz, in a range that does not unequivocally allow distinguishing between Rh(I) and Rh(III). The two coordinated carbon atoms are detected at 44.7 ($^1J_{CRh}$ = 15.5 Hz) and 59.6 ($^1J_{CRh}$ = 13.8 Hz) ppm by ^{13}C NMR spectroscopy. The small coupling constants of all aromatic carbon atoms (smaller than 9 Hz) prove that no activation analogous to **2** has taken place (not even at elevated temperature,[10] Scheme 3). In **2** the $^1J_{CRh}$ for the carbon/rhodium bond of the five-membered ring is larger than 40 Hz.

We do have an X-ray structure with η^2-CO-coordination applying **L2** to Ru(NO)Cl(PPh_3)$_2$ in hand, which will be published in the context of another article.

X-ray Structure, Spectroscopic Results, and Orbital Shape of the Activated Complex. For complex **2a** crystals suitable for X-ray analysis could be grown from diethyl ether/hexane. A depiction of a structure in the solid state is shown in Figure 4.

The C−C single bond between C7 and C8 is completely broken (distance C7−C8: 2.77 Å). A five-coordinated T-shaped structure (pseudo-Jahn−Teller effect) is obtained with the acyl ligand *trans* to the free coordination site, as would have been predicted by the strength of *trans* influences of the different ligands.

In ^{13}C NMR spectroscopy the two carbon atoms connected to Rh in **2b** appear at 198.1 ppm ($^1J_{CRh}$ = 28.8 Hz, acyl moiety) and 122.4 ppm ($^1J_{CRh}$ = 40.4 Hz, phenyl moiety), in accordance with a complete and permanent cleavage of the C−C single bond in solution as well. In the ^{31}P NMR spectroscum of **2a** two doublets of doublets are detected at 152.3 ppm ($^1J_{PRh}$ = 130.7 Hz) and 172.9 ppm ($^1J_{PRh}$ = 127.7 Hz) with a $^2J_{PP}$ coupling constant of

Scheme 2

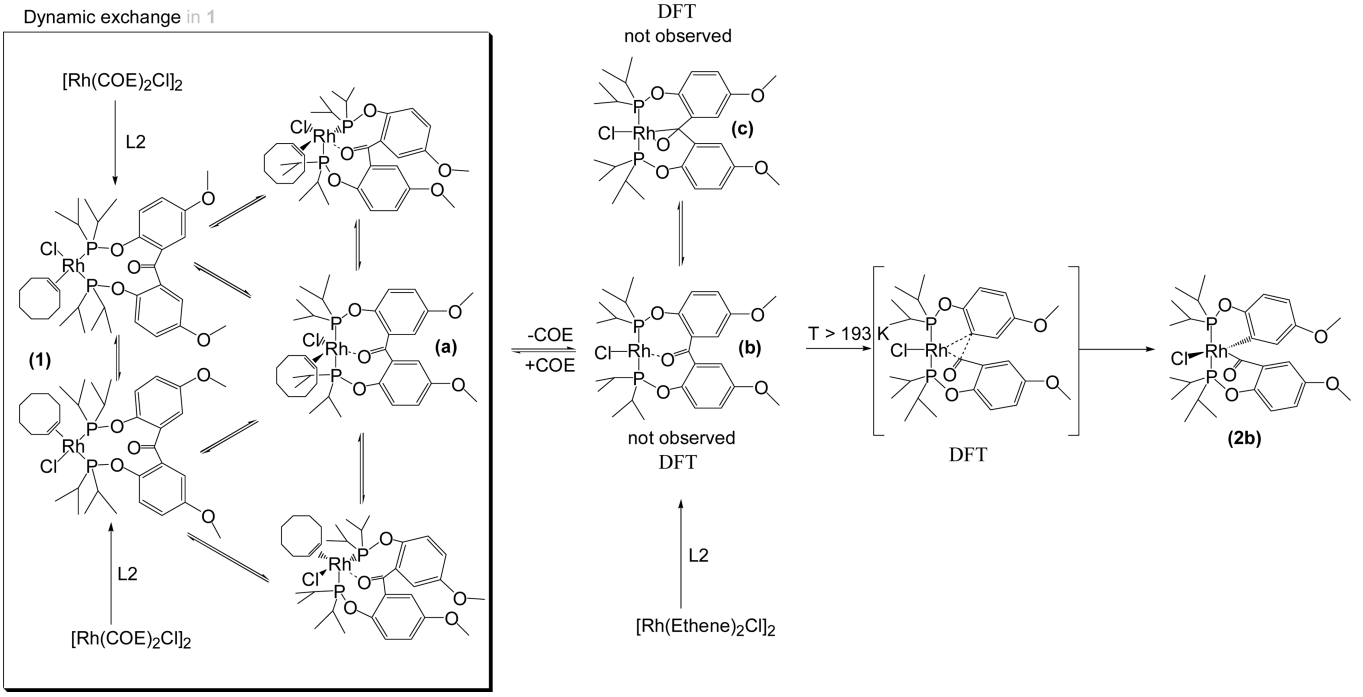

Scheme 3

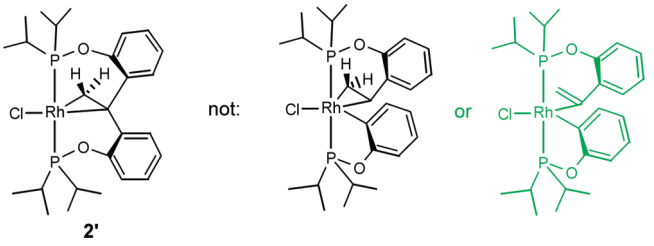

395 Hz, proving the *trans* configuration of the two P atoms. The $^{1}J_{PRh}$ coupling constants show values at the borderline between Rh(I) and Rh(III). The ν(CO) wavenumber is found at 1655 cm^{-1}, supporting that no further interaction takes place between the Rh center and the carbonyl oxo group, in accordance with the X-ray analysis data.

We want to stress the special electronic and orbital situation in **2** because it will be crucial to understand not only its structure but also its reactivity toward Lewis bases.

The geometry distortion from a trigonal-bipyramidal structure toward a square-pyramidal one is brought about by a pseudo-Jahn−Teller effect. This leads to the free coordination site *trans* to the acyl ligand (Scheme 4). It is important to understand that this coordination site is not very attractive to a Lewis base because the LUMOs of the complex are ligand- rather than metal-centered (Scheme 5). Because of the π-acidity of the two phosphorus ligands, the d_{xz}-HOMO orbital is not ideally suited for an interaction with an external π-acceptor approaching the free coordination site either. This is the reason that the free coordination site remains unoccupied even in the presence of Lewis bases such as acetonitrile and pyridine.

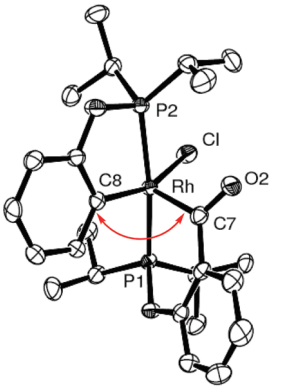

Figure 4. ORTEP representation of a molecule in the solid state of compound **2a**. Thermal ellipsoids are given at the 50% probability level. Hydrogen atoms are omitted for clarity. Selected bond lengths (Å) and angles (deg): d(C8−Rh) = 2.062(3), d(C7−Rh) = 1.958(3), d(C7−C8) = 2.770(4), d(P1−Rh) = 2.2784(7), α(C8−Rh−C7) = 87.07(11), α(C8−Rh−CL) = 160.82(7), α(C7−Rh−CL) = 110.51(8), α(P1−Rh−P2) = 170.95(3).

DFT Calculations on the C−C Single Bond Activation. Scheme 6 shows the LUMO and the LUMO+1 of **2a** calculated by DFT at the LanL2DZ/B3PW91 level. These calculations support the qualitative description demonstrated in Scheme 5.

We also examined the reaction Scheme 2 by DFT calculations, in particular the activation step of the C−C single bond (Scheme 7). The results of the calculations support an η^2-CO-coordinated intermediate as the most stable structure and as a resting state, which via an η^1-O-intermediate forms an η^2-CC transition state. This development would be in accordance with the negative activation entropy found experimentally. According

dx.doi.org/10.1021/om200288e |*Organometallics* 2011, 30, 4039–4051

Scheme 4

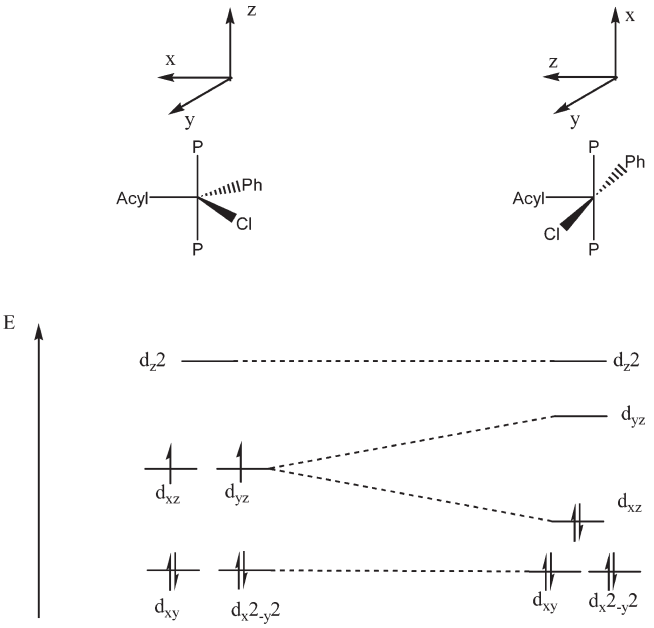

Scheme 5

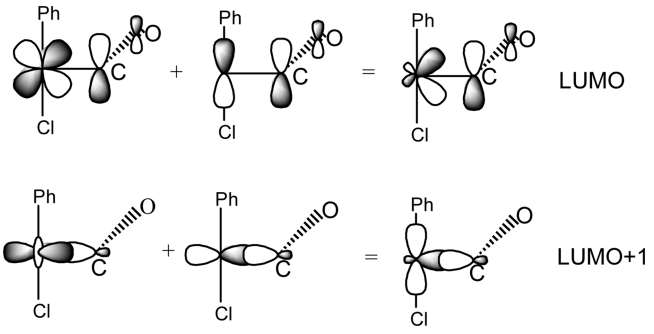

to the calculations, an η^3-CCO transition state, which would also account for a negative activation entropy, is less favored in comparison to the η^2-CC route (too high activation barrier). The calculations predict correctly that the quantitative bond cleavage is thermodynamically favored in comparison to the nonactivated η^2-CO complex.

Further Fate of the Activated Complex: Migratory Extrusion. On dissolving crystals of **2a** in chloroform or toluene (two sets of doublets of doublets), the occurrence of a further signal (compound **3a**, broad doublet, 174.0 ppm, $^1J_{RhP}$ = 71.3 Hz ⟹ Rh^{III}) in the $^{31}P\{^1H\}$ NMR is observed. If the solution is cooled to 231 K, the signal sharpens and an increase in intensity is observed in $CDCl_3$. Figure 5 shows this change over the temperature range between 213 and 303 K.

A carbonyl signal (2048 cm^{-1} ⟹ Rh(III)) can be detected by IR spectroscopy when **2a** is dissolved in chloroform or toluene.[11] It was further proven by 2D EXSY spectroscopy that a connection exists between compounds **2a** and **3a** and that these two compounds convert slowly into each other (Figure 6).

The $^{31}P\{^1H\}-^{31}P\{^1H\}$ phase-sensitive 2D exchange spectrum unambiguously proves the chemical exchange between P_A, P_B, and P_C using mixing times larger than 250 ms (all peaks appearing with the same phase as the diagonal elements). It has to be mentioned that no chemical exchange between the three P atoms P_A, P_B, and P_C can be observed and only very weak NOE signals are found if a mixing time of only 125 ms is applied. From this an approximate exchange rate smaller than 4 Hz at 293 K can be estimated. We explain the chemical exchange by a migratory extrusion/insertion of the carbonyl moiety, as illustrated in Scheme 8.

Scheme 6

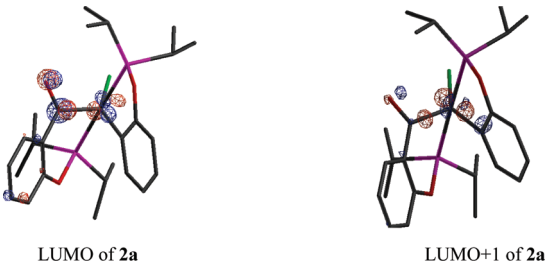

Scheme 7

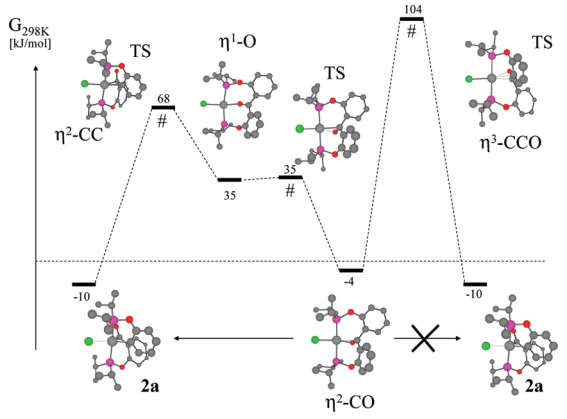

A structure analogous to **3a** for Ir was found by us and was analyzed by X-ray diffraction in another paper.[8]

Since we can detect the terminal metal carbonyl moiety in IR spectroscopy on one hand and no further compounds can be detected by ^{31}P NMR spectroscopy on the other hand, an exchange of P_A and P_C via carbonyl-coordinated complex **3′** can be excluded as the ground-state structure. From Figure 5 the equilibrium constant for the migratory extrusion/insertion reaction can be measured at various temperatures and a van't Hoff plot can be generated (Figure 7).

From the van't Hoff plot an enthalpy of 9.3 ± 0.5 kJ/mol and an entropy of 53.8 ± 1.8 J/(mol K) are extracted for the reaction **3a** → **2a**. Thus, the entropic gain is the driving force for the formation of **2a**. We mention that in the solid-state structure the coordination sites *cis* to the migrating phenyl ring are occupied, and thus some kind of rearrangement must take place in advance of the migratory extrusion.

In the case of **2b** (*para*-OMe substituents) no migratory extrusion/insertion is observed. We propose that increasing the σ-donor strength of the aryl groups shifts the equilibrium completely in favor of the acyl complex.

dx.doi.org/10.1021/om200288e |*Organometallics* 2011, 30, 4039–4051

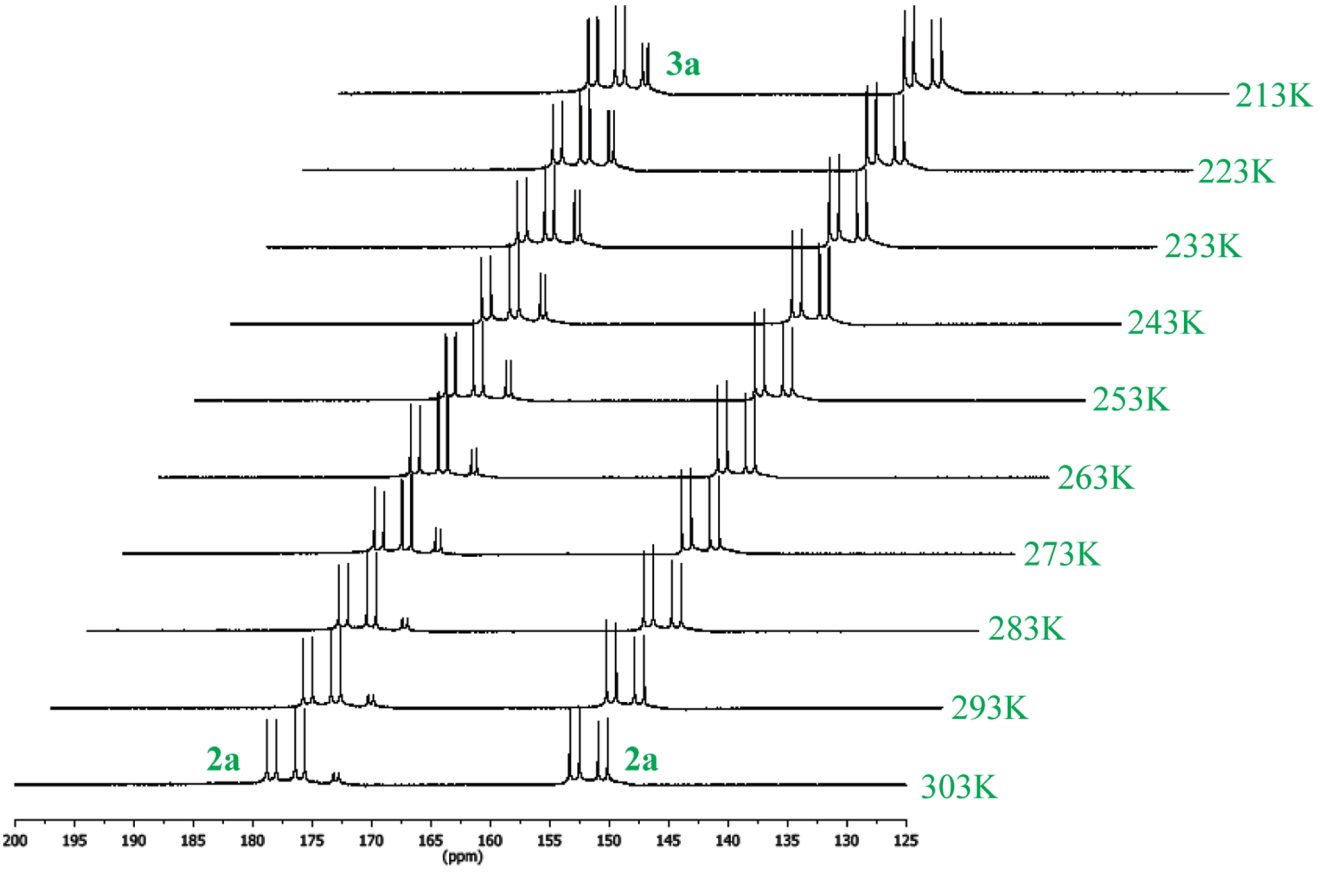

Figure 5. Detection of compound **3a** by $^{31}P\{^{1}H\}$ NMR spectroscopy in $CDCl_3$ at various temperatures. NMR spectra were recorded in 10 K steps between 213 K (top) and 303 K (bottom).

Further Fate of the Activated Complex: Reductive Elimination. The stability of **2a**/**b** in solution is highly concentration- and temperature-dependent. Both compounds react further on heating to 343 K within 150 min in toluene (or using concentrations above 0.08 mol/L even at room temperature; Figure 8 and Scheme 9).

The final product **7** showed up as a slightly broadened doublet at 158.8 ppm in the $^{31}P\{^{1}H\}$ NMR spectrum with $^{1}J_{RhP}$ = 133.7 Hz. IR spectroscopy revealed a characteristic absorption for a terminal metal carbonyl at 1971 cm^{-1} (supporting Rh(I)). The material was hardly soluble in common organic solvents and showed broad resonances in ^{1}H and $^{13}C\{^{1}H\}$ NMR spectra using $CDCl_3$ as solvent. We propose on the basis of these observations as the major product the ligand-bridged coordination polymer **7** of *trans* $Rh^{(I)}(CO)(Cl)$ units (Scheme 9).

Thus, CO extrusion followed by reductive elimination of two C_{aryl}—Rh bonds must have occurred. A concerted reductive elimination demands a *cis* configuration of the participating aryl groups in the prior stage. Attempts to synthesize monomeric species of **6** (Scheme 9) starting with *trans*-$Rh(CO)(Cl)(PPh_3)_2$ and the corresponding biphenyl ligand resulted in the formation of **7** (heating **7** with excess PPh_3 did not liberate the free biphenyl ligand from the rhodium). The ligand backbone seems to be too short for strain-free coordination in a *trans* fashion. Two further species, **4** and **5**, are observed on the pathway to **7**. The nature of compounds **4** and **5** is inferred (*inter alia*) through the magnitude of the phosphorus—phosphorus and rhodium—phosphorus coupling constants (Figure 8: two doublets of doublets each).

In both compounds the phosphorus moieties are connected to a rhodium(III) center (**5**: 159.9 ppm with $^{1}J_{RhP}$ = 83.2 Hz, 167.9 ppm with $^{1}J_{RhP}$ = 109.9 Hz; **4**: 167.6 ppm with $^{1}J_{RhP}$ = 68.0 Hz, 181.0 ppm with $^{1}J_{RhP}$ = 131.1 Hz) and are located *cis* to one another (**5**: $^{2}J_{PP}$ =23.8 Hz; **4**: $^{2}J_{PP}$ = 13.1 Hz).

The fairly large coupling constant of the phosphorus in the five-membered ring (larger chemical shift than the six-membered-ring phosphorus) in **4** supports the free coordination side *trans* to it.

5 reacts slower in a reductive elimination than **4′** and is thus observable, because the two phenyl moieties to be eliminated are orthogonal to each other. We state that the analogous Ir complex (X-ray analysis in ref 8) is stable against reductive elimination, and the analogue to **4′** (X-ray analysis in ref 8) reacts thermally into **5**.

Further Fate of the Activated Complex: Coordination of Lewis Bases. The activated complex **2a**/**b** with free (and in the first place innocent) coordination site was also reacted with several Lewis bases such as CO, ^{13}CO, *tert*-butyl isonitrile, pyridine, acetonitrile, and ^{15}N-acetonitrile. Scheme 10 summarizes the results found.

Treatment of **2a** with carbon monoxide ($CDCl_3$ or toluene, 1.7 bar CO) allows the connection to the closely related Ir system starting with Vaska's complex. Although the intermediate **8** was not observed, we were able to isolate the analogous Ir compound.[8] A ketone coordination in a η^2-C,O fashion seems not to play a role in **9** in analogy to Ir since this is expected to prevent the formation of coordination polymer **10**. No exchange between

dx.doi.org/10.1021/om200288e |*Organometallics* 2011, 30, 4039–4051

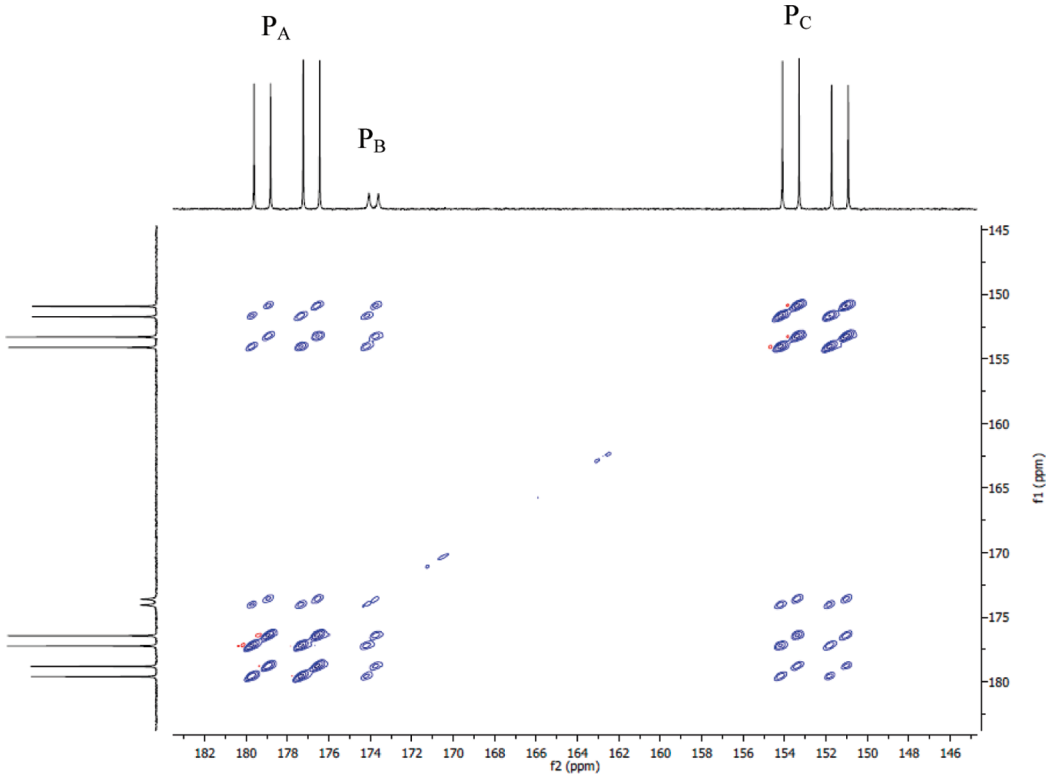

Figure 6. $^{31}P-^{31}P$ EXSY spectrum of **2a**/**3a** at 298 K in $CDCl_3$ (18 mg/0.5 mL). t_1 = 5.0 s and τ_m = 250 ms.

Scheme 8

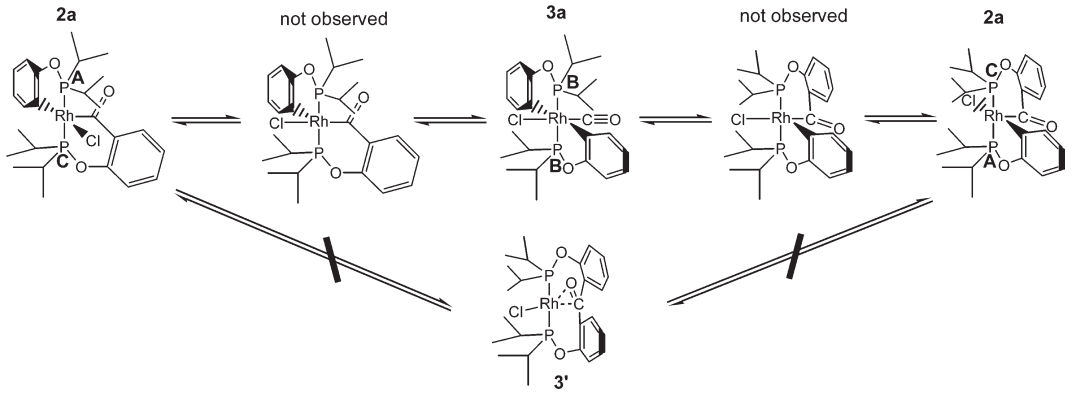

the carbonyl of the acyl position and the incoming carbon monoxide is observed (proved by ^{13}CO labeling). We propose that the ease with which reductive elimination occurs on treating **2a** with carbon monoxide (at room temperature in 20 min) is not only due to the π-accepting nature of CO (promoting the formation of rhodium(I)) but also due to the participation of the acyl-oxygen in the transition state (κ^1-O interaction). Attempts to synthesize monomeric species of **9** starting with $Rh(CO)(Cl)(PPh_3)_2$ and the corresponding benzophenone ligand resulted in the formation of the final product **10**. Changing the precursor to $[Rh(CO)_2Cl]_2$ had no effect concerning the formation of **10** rather than **9**.

Again the decisive role of the ligand backbone length becomes obvious. A hardly soluble coordination polymer of *trans* Rh(I)-(CO)(Cl) units (**10**) is finally obtained ($^{31}P\{^1H\}$ NMR: 165.8 ppm (d, $^1J_{PRh}$ = 133.7 Hz)). IR spectroscopy showed signals at 1977 and 1671 cm^{-1}, which are assigned to the metal-bonded terminal carbonyl at a Rh(I) center and the ketone moiety. This reaction path allows a direct comparison of the behavior between Rh and Ir. While the Ir complex analogous to **8** is stable and isolable and shows a reaction sequence of CO loss (via the analogue to **2a**, which is not stable in the case of Ir), carbonyl extrusion, and *trans*/*cis* isomerization on thermal treatment, in the case of Rh the complex **2** is stable and the reaction sequence develops in the opposite direction via CO coordination and reductive elimination. We propose that the stronger metal carbon bonds in the case of Ir are at least part of the reason for this complementary behavior.

Using *tert*-butyl isonitrile (weaker π-acceptor compared to CO) allows the observation of the 6-fold-coordinated species in

dx.doi.org/10.1021/om200288e |*Organometallics* 2011, 30, 4039–4051

the case of **2b** in benzene. Only one isomer (from two possible diasteromeric forms) is observed. The change in $^{2}J_{PP}$ and $^{1}J_{RhP}$ coupling constants (373.1 Hz; 148.0 ppm with 114.4 Hz and 178.5 ppm with 116.8 Hz, respectively) in comparison to **2b** clearly shows the increase of the coordination number at constant configuration of the P atoms and constant oxidation state +III of Rh. The resulting compound decomposed within several hours at room temperature.

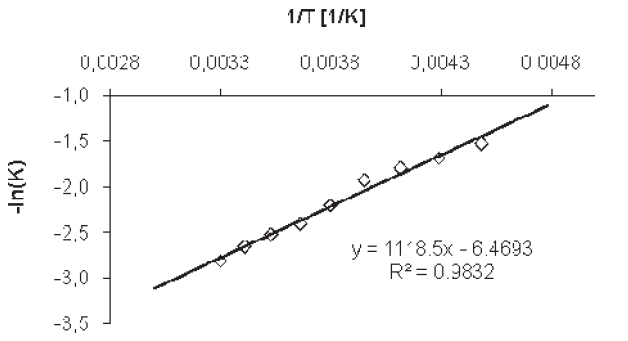

Figure 7. van't Hoff plot for the equilibrium **3a** → **2a**.

The behavior of **2a** in coordinating solvents (pyridine and acetonitrile) is elusive. Figures 9 and 10 show the dynamic behavior of **2a** between 233 and 313 K in pyridine/303 K in acetonitrile. In both solvents neither **3a** nor **5** (Scheme 9) is observed. At 233 K two major species can be detected in both solvents in a ratio of 1.3:1 (**2a**/**2a**$_{solv}$). Rather similar chemical shift values and coupling constants are found (e.g., major diasteromer in acetonitrile at 233 K: $^{2}J_{PP}$ = 374.2 Hz, $^{1}J_{RhPA}$ = 115.9 Hz, and $^{1}J_{RhPB}$ = 124.7 Hz, comparable to the *tert*-butyl isonitrile adduct of **2b**). At higher temperatures in acetonitrile (303 K) only one set of signals for **2a** is seen due to the expected time-averaged fast solvent coordination−decoordination. This behavior is completely reversible for **2a**, whereas the formation of a second compound (**4**$_{solv}$) under the investigated conditions is an irreversible process (**2a**$_{solv}$ completely disappears after ∼30 min at 353 K in pyridine accompanied by the formation of

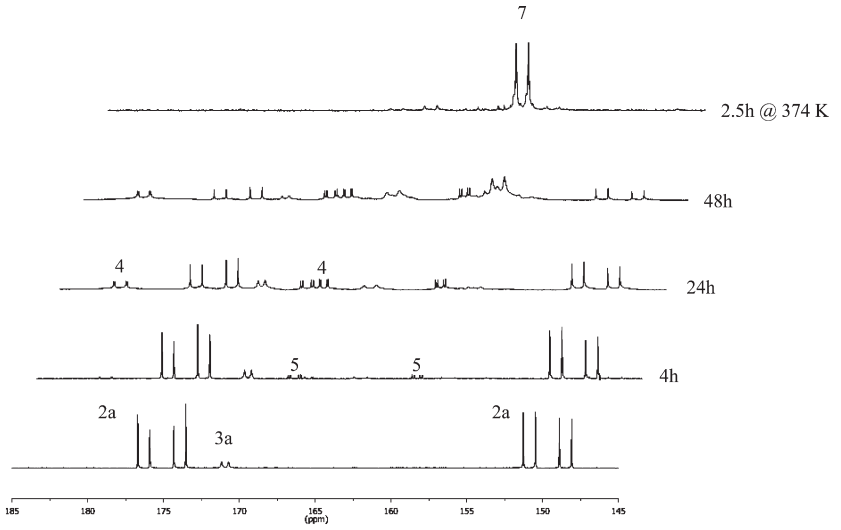

Figure 8. Further reaction on thermal treatment of **2a** followed by ^{31}P NMR spectroscopy at different time stages.

Scheme 9

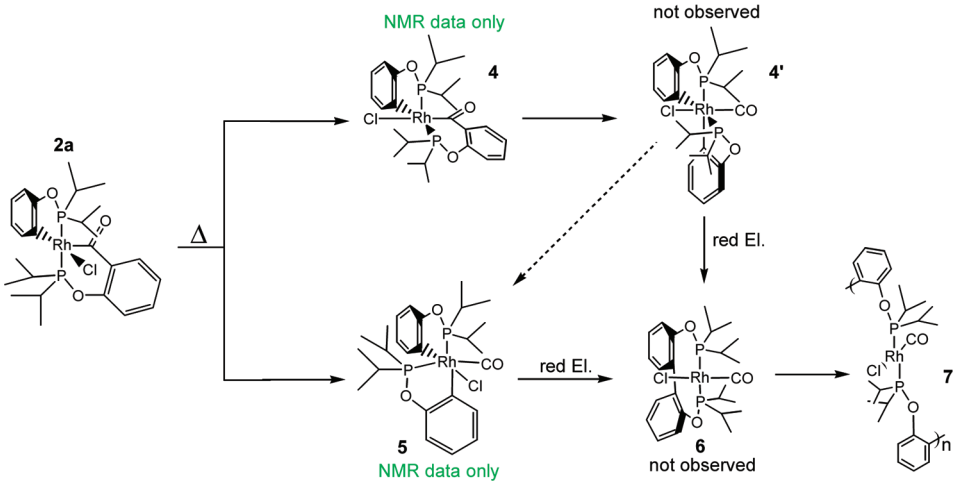

dx.doi.org/10.1021/om200288e |*Organometallics* 2011, 30, 4039–4051

Scheme 10

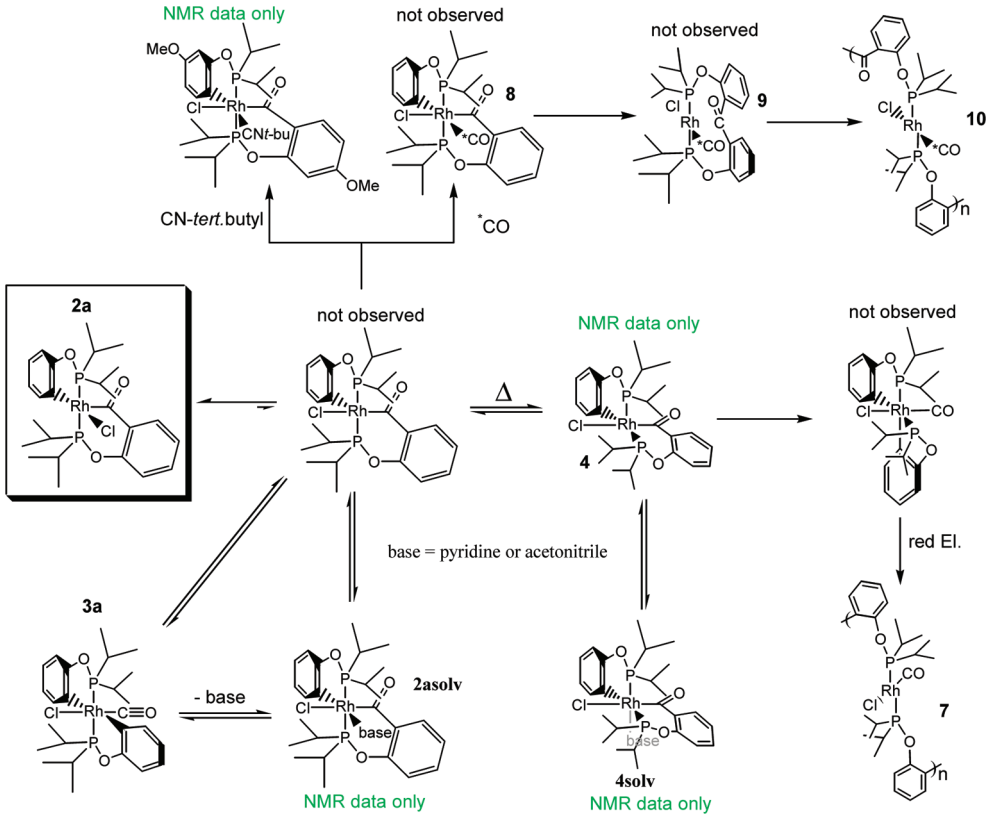

the reductive elimination product **7**). A slow isomerization of **2a** to **4** (Scheme 9) is proposed to account for this behavior, which is also seen on the pathway to **7**.

As can be seen from Figures 9 and 10, the six-membered ring (smaller chemical shift) is more strongly influenced by the coordination of the solvent than the five-membered ring (larger chemical shift). This is in accordance with the proposed equilibrium **2** + solv → $\mathbf{2_{solv}}$ since for the phosphorus in the five-membered ring almost nothing changes through the coordination of the solvent (exchange Cl vs solvent molecule), while the isopropyl groups of the phosphorus atom in the six-membered ring are perturbated by the shifted Cl ligand vs a free coordination site before the solvent coordination.

To further prove that the coordinating influence of the solvent molecules is responsible for the observed dynamic process, ^{15}N studies were undertaken. The end-on coordination via the N atom in the case of acetonitrile is assumed due to the similarity to the behavior in pyridine (*vide supra*). A combination of isotopomers $CD_3CN/CH_3C^{15}N$ as solvent was tested. No coupling ($^2J_{PN}$) between ^{31}P moieties and the ^{15}N nuclei of acetonitrile was observed using $^{31}P\{^1H\}$ NMR spectroscopy at 293 K or at 233 K (which were expected to be about $^2J_{PNcis}$ = 2−6 Hz and $^2J_{PNtrans}$ = 20−40 Hz). No change of the line shape of the acetonitrile signal on going from low to high temperatures in ^{15}N NMR spectra (−136.9 ppm, singlet; sweep width: 30 to −670 ppm) was observed (25 mg/0.4 mL metal complex was used). As had been already mentioned, no **3a** is observed.

The solvent combination $C_7D_8/CH_3C^{15}N$ (∼10/1) was further used in order to have the possibility to measure at lower temperatures and exclude the competition $CD_3CN/CH_3C^{15}N$. No splitting of the $^{31}P\{^1H\}$ NMR signals due to coupling to ^{15}N nuclei was found in the temperature range 193−293 K. The observed dynamic process on the ^{31}P NMR time scale is completely reversible, although in this case the signals for **3a** are observable over the whole temperature range and sharpen on lowering the temperature without change of the $^1J_{RhP}$ = 72.4 Hz coupling constant. While in acetonitrile two diastereomeric structures can be frozen out at 233 K, only one set of sharp signals is observed at 203 K in this solvent mixture.

Coupling to ^{15}N nuclei is not observed due to the magnitude of the potential $^2J_{PN}$ coupling constant, which is expected to be only large enough in the case of a phosphorus−nitrogen *trans* position ($J \approx 40$ Hz expected for a *trans* configuration). The ^{15}N NMR spectrum at 213 K did not show a further signal besides that for the solvent peak (sweep width: 30 to −670 ppm).

Due to the unfavorable overlap and broadening of some signals, reliable integration is excluded to decide whether the equilibrium constant ($\mathbf{2a_{solv}}/\mathbf{3a}$) has changed or not compared to pure toluene. It seems difficult to find a compromise between enough coordinating solvent molecules to influence the anticipated equilibrium on one hand and observing coordinated acetonitrile units at the metal center using ^{15}N NMR spectroscopy on the other (assuming practicable measuring times at low temperatures). Additionally, ^{15}N NMR signals can possibly show a coupling to the ^{103}Rh metal center and two nonequivalent ^{31}P moieties, which results in a further splitting of the signal intensity.

$^{13}C\{^1H\}$ NMR spectroscopy experiments in pyridine at room temperature and $^{13}C\{^1H\}$ NMR spectroscopy experiments in acetonitrile at 233 K showed only broad signals without resolution

dx.doi.org/10.1021/om200288e |*Organometallics* 2011, 30, 4039–4051

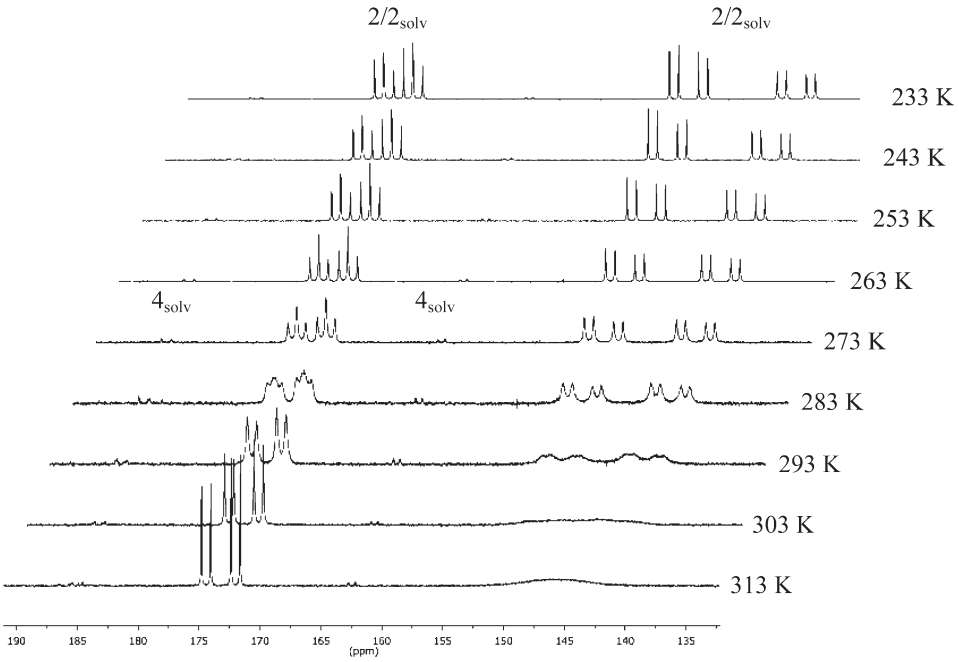

Figure 9. Dynamic behavior of **2a** in pyridine-d_5 followed by $^{31}P\{^1H\}$ NMR spectroscopy. NMR spectra were recorded in 10 K steps between 233 K (top) and 313 K (bottom).

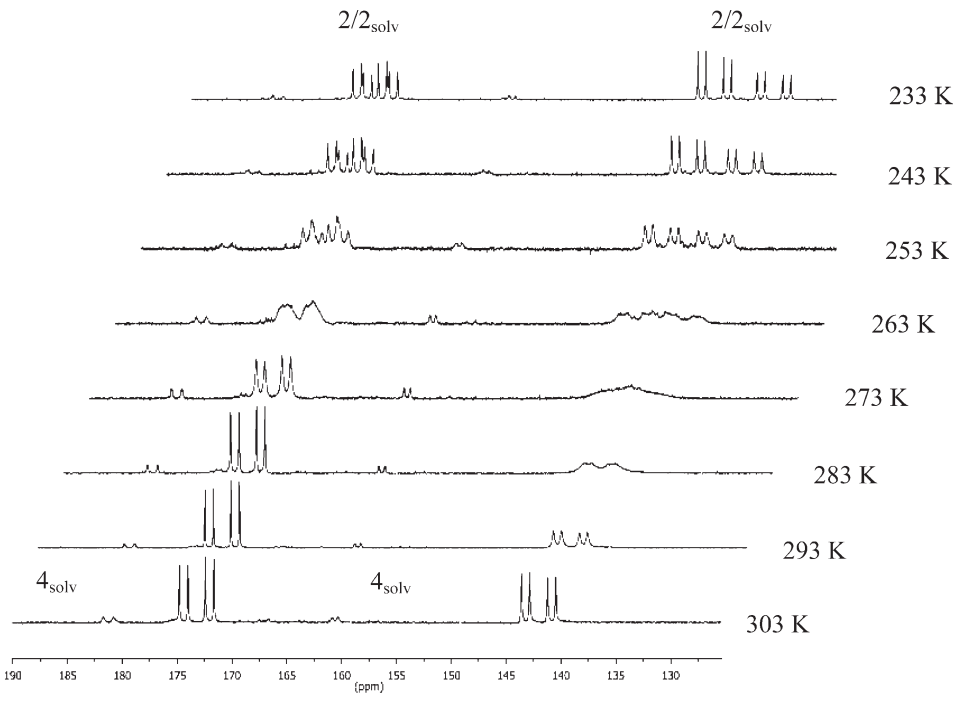

Figure 10. Dynamic behavior of **2a** in acetonitrile followed by $^{31}P\{^1H\}$ NMR spectroscopy. NMR spectra were recorded in 10 K steps between 233 K (top) and 303 K (bottom).

of signal multiplicities, which would allow the determination of geometry, revealing coupling constants.

Summary. We were able to cleave a C−C single bond quantitatively at 193 K. To the best of our knowledge, this is the lowest temperature under which this kind of reaction has ever been observed. We were able to explain and quantify the kinetics and the mechanism behind this reaction and to support the quantitative experimental results by DFT calculations. We were also able to elucidate the further fate of the activated complex and its reactions with Lewis bases.

EXPERIMENTAL SECTION

General Procedures. Manipulations and experiments were performed under an argon atmosphere using standard Schlenk techniques and in an argon-filled glovebox if not otherwise stated. Diethyl ether,

dx.doi.org/10.1021/om200288e |*Organometallics* 2011, 30, 4039–4051

pentane, dichloromethane, and toluene were dried and degassed using a two-column drying system (MBraun) and stored under an argon atmosphere over molecular sieves. Deuterated solvents used in NMR studies, including $CDCl_3$, CD_2Cl_2, benzene-d_6, toluene-d_8, nitromethane-d_3, pyridine-d_5, and acetontrilie-d_3, were stored under argon over molecular sieves. $RhCl_3 \cdot H_2O$ and $[Rh(ethene)_2Cl]_2$ were purchased from Strem. $[RhCl(coe)_2]_2$,[12] $Rh(CO)Cl(PPh_3)_2$,[13] and $[Rh(CO)_2Cl]_2$[14] were prepared according to literature methods. Carbon monoxide 2.5 was purchased from Messer Griessheim. ^{13}C-Labeled CO (^{13}CO, 99%; <2% ^{18}O) was purchased from Buchem BV (The Netherlands). Both were used without further purification.^{15}N-Labeled acetonitrile was synthesized by reaction of acetyl chloride with $^{15}NH_4Cl$ (98% ^{15}N, Aldrich), followed by dehydration of the amide with P_4O_{10} at 80 °C. 2,2′-Dihydroxo-4,4′-dimethoxobenzophenone and 2,2′-dihydroxobenzophenone were purchased from Merck or Aldrich and used without further purification. Diisopropylphosphine chloride was purchased from Aldrich and was not further purified. The NMR measurement was performed on a Bruker AMX400 or Mercury plus 400 high-resolution system (Fa. Varian Deutschland GmbH). ^{1}H NMR (400 MHz) and ^{13}C NMR (100 MHz) chemical shifts are given in ppm relative to the solvent signal for $CDCl_3$ (7.26 and 77.0), CD_2Cl_2 (5.32 and 54.0), C_6D_6 (7.15 and 128.0), C_7D_8 (2.09 and 20.4), and nitromethane-d_3 (4.28 and 61.2). ^{31}P NMR (161 MHz) used 85% H_3PO_4 as an external standard. Elemental analyses were carried out by the Microanalytical Laboratory of the Technische Universität München. Mass spectra were acquired by the Technische Universität München Mass Spectrometry Laboratory using a Finnigan MAT 90 spectrometer equipped with a FAB ionization chamber. The FTIR spectra were measured on a JASCO FI7IR-460plus spectrometer using KBr pellets or on a Nexus FT-IR spectrometer with an ATR (attenuated total reflectance) unit (Fa. Thermo (Nicolet) Elektron Spectroscopy GmbH).

Ligands **L1** and **L2** were synthesized according to the previously reported literature methods.[8]

Crystal Structure Analysis. Preliminary examination and data collection were carried out on a κ-CCD device (Oxford Diffraction Xcalibur3) with an Oxford Instruments cooling system with graphite-monochromated Mo Kα radiation (λ = 0.71073 Å). Data collection was performed at 150 K. Raw data were corrected for Lorentz, polarization, and, arising from the scaling procedure, latent decay and absorption effects. After merging independent reflections remained and all were used to refine the parameters. The structure was solved by a combination of direct methods and difference Fourier syntheses.[15] All non-hydrogen atoms were refined with anisotropic displacement parameters. All hydrogen atoms were placed in calculated positions and refined using a riding model. Full-matrix least-squares refinements were carried out by minimizing $\Sigma w(F_o^2 - F_c^2)^2$ and converged. The final difference Fourier maps showed no striking features.

DFT Calculations. The DFT calculations were performed using the program suite Gaussian 03.[16] All molecular geometries were fully optimized. Transition states were obtained using the OPT2 or OPT3 function implemented in the program suite and were proven to be one-dimensional saddle points by frequency analysis in each case. The DFT method used includes Becke's three-parameter hybrid exchange functional in combination with the correlation functional of Perdew and Wang (B3PW91). Geometry calculations and frequency calculations were performed using the valence double-ζ LANL2DZ basis set.

Isolation of 2a and 2b. A 72 mg (0.10 mmol, 1 equiv) amount of $[Rh(coe)_2Cl]_2$ is dissolved in 10 mL of toluene. Then 95 mg (0.21 mmol, 2.1 equiv) of the benzophenone ligand **L1** is dissolved in the same volume and added slowly via cannula to the first. After stirring for 2 h at room temperature the solution (sometimes suspension) is filtered and the solvent evaporated *in vacuo*. A brown oil is obtained, which upon washing twice with 2 mL of cold hexane and 1.5 mL of cold diethyl ether yields 76 mg of a yellow-orange powder (crude yield: 65%). Cooling a saturated diethyl ether/hexane (5/2) solution of **2a** overnight to 241 K delivers yellow crystals of **2a** exclusively (yield: 55%). For this reaction it is highly recommended to use the freshly prepared ligand **L1** (otherwise the formation of an insoluble precipitate was observed, which decreases the yield).

In the case of **2b**, a greenish oil is received, which is dissolved in hexane and transferred into a small column (Pasteur pipet) with 5 cm of aluminum oxide. Then 10 mL of hexane are flashed through. After that 7 mL of diethyl ether is flashed through the column to regain after evaporation a light yellowish-green solid (crude yield: 80%). **2b** can be crystallized from hexane/diethyl ether (241 K) (1/2), resulting in yellow crystals (yield: 50%).

***trans*-Rh(Cl)(κ^2-*P*,*C*-P(OC$_6$H$_4$)-(^{i}C$_3$H$_7$)$_2$)(κ^2-*P*,*C*$_{acyl}$-P(OC$_6$H$_4$CO)-(^{i}C$_3$H$_7$)$_2$) (2a).** ^{1}H NMR (C_6D_6, rt, ppm): 1.04 (6H, pseudo quin, $^3J_{HH}$ = 7.32 Hz, $^3J_{PH}$ = 12.28 Hz, CHCH_3), 1.13 (3H, dd, $^3J_{HH}$ = 7.36 Hz, $^3J_{PH}$ = 14.68 Hz, CHCH_3), 1.27 (3H, dd, $^3J_{HH}$ = 7.36 Hz, $^3J_{PH}$ = 17.17 Hz, CHCH_3), 1.32 (3H, dd, $^3J_{HH}$ = 7.36 Hz, $^3J_{PH}$ = 17.17 Hz, CHCH_3), 1.37 (3H, dd, $^3J_{HH}$ = 7.36 Hz, $^3J_{PH}$ = 15.93 Hz, CHCH_3), 1.57 (3H, dd, $^3J_{HH}$ = 7.36 Hz, $^3J_{PH}$ = 14.72 Hz, CHCH_3) 1.71 (3H, dd, $^3J_{HH}$ = 6.12 Hz, $^3J_{PH}$ = 15.93 Hz, CHCH_3), 2.73 (2H, sept, $^3J_{HH}$ = 7.36 Hz, CHCH$_3$), 3.19 (2H, dsept, $^2J_{PH}$ = 2.44 Hz, $^3J_{HH}$ = 7.36 Hz, CHCH$_3$), 6.32 (pseudo sept, 1H, $^3J_{HH}$ = 8.12 Hz, $^3J_{HH}$ = 5.95 Hz, $^4J_{HH}$ = 2.76 Hz, H$_{arom}$), 6.58 (td, 1H, $^3J_{HH}$ = 7.36 Hz, $^4J_{HH}$ = 1.46 Hz, H$_{arom}$), 6.76 (pseudo t, 1H, $^3J_{HH}$ = 7.36 Hz, H$_{arom}$), 6.83−6.84 (m, 2H, H$_{arom}$), 6.89 (d, 1H, $^3J_{HH}$ = 7.54 Hz, H$_{arom}$), 7.09 (d, 1H, $^3J_{HH}$ = 7.36 Hz, H$_{arom}$), 7.56 (d, 1H, $^3J_{HH}$ = 7.36, H$_{arom}$). ^{13}C{^{1}H} NMR ($CDCl_3$, rt, ppm): 15.93 (s, CHCH_3), 16.32 (s, CHCH_3), 16.35 (s, CHCH_3), 16.82 (s, CHCH_3), 18.25 (s, CHCH_3), 18.51 (s, CHCH_3), 19.19 (s, CHCH_3), 19.29 (d, $^2J_{CP}$ = 4.61 Hz, CHCH_3), 29.24 (d, $^1J_{CP}$ = 17.82 Hz, CHCH_3), 29.44 (d, $^1J_{CP}$ = 23.75 Hz, CHCH_3), 29.74 (d, $^1J_{CP}$ = 23.76 Hz, CHCH_3), 29.97 (d, $^1J_{CP}$ = 23.76 Hz, CHCH_3), 112.05 (d, $^3J_{CP}$ = 14.85 Hz, CH_{arom}, DEPT), 120.25 (s, CH_{arom}, DEPT), 121.22 (s, CH_{arom}, DEPT), 122.52 (s, CH_{arom}, DEPT), 125.71 (s, CH_{arom}, DEPT), 127.69 (d, $^3J_{CP}$ = 11.88 Hz, CH_{arom}, DEPT), 133.18 (s, CH_{arom}, DEPT), 141.18 (s, CH_{arom}, DEPT), 155.23 (s, COP), 167.58 (d, $^2J_{CP}$ = 14.85 Hz, COP), 203.48 (dd, $^1J_{RhC}$ = 29.70 Hz, $^2J_{CPcis}$ = 8.90 Hz, RhCO_{Acyl}). ^{13}C{^{1}H} NMR ($CDCl_3$, 213K, ppm): 124.76 (dd, $^3J_{CP}$ = 18.64 Hz, $^2J_{RhC}$ = 3.27 Hz, C$_{arom}$), 134.85 (dd, $^1J_{RhC}$ = 42.86 Hz, $^2J_{CPcis}$ = 3.27 Hz, RhC$_{Aryl}$). ^{31}P{^{1}H} NMR ($CDCl_3$, rt, ppm): 152.25 (dd, $^2J_{PP}$ = 395.02 Hz, $^1J_{RhP}$ = 130.68 Hz), 172.93 (dd, $^2J_{PP}$ = 395.02 Hz, $^1J_{RhP}$ = 127.72 Hz). IR (ATR) [cm^{-1}]: 1655 (CO_{Acyl}). MS (FAB, *m*/*z*): 584 [M] (21%) with correct isotopic pattern for $C_{25}H_{36}ClO_3P_2Rh$, 556 [M − CO] (100%) with correct isotopic pattern for $C_{24}H_{36}ClO_2P_2Rh$, 549 [M − Cl] (94%) with correct isotopic pattern for $C_{25}H_{36}O_3P_2Rh$. Anal. Calcd for $C_{25}H_{36}ClO_3P_2Rh$: C: 51.34, H: 6.20. Found: C: 51.51, H: 5.93.

***trans*-(CO)(Cl)Rh(κ^2-*P*,*C*-P(OC$_6$H$_4$)-(^{i}C$_3$H$_7$)$_2$)$_2$ (3a).** ^{31}P{^{1}H} NMR ($CDCl_3$, rt, ppm): 173.95 (br d, $^1J_{RhP}$ = 71.26 Hz). IR (KBr pellet) [cm^{-1}]: 2048 ($CO_{Carbonyl}$). Equilibrium ratio of **2a**/**3a**: 17/1 ($CDCl_3$, 303 K), 13/1 (toluene, 303 K). ^{1}H and ^{13}C{^{1}H} NMR signals were too weak for a complete assignment.

***trans*-Rh(Cl)(κ^2-*P*,*C*-P(O-*p*-OCH$_3$-C$_6$H$_3$)-(^{i}C$_3$H$_7$)$_2$)(κ^2-*P*,*C*$_{acyl}$-P(O-*p*-OCH$_3$-C$_6$H$_4$CO)-(^{i}C$_3$H$_7$)$_2$) (2b).** ^{1}H NMR (C_6D_6, ppm): 1.09 (6H, dd, $^3J_{HH}$ = 7.36 Hz, $^3J_{PH}$ = 12.26 Hz, CHCH_3), 1.19 (3H, dd, $^3J_{HH}$ = 7.36 Hz, $^3J_{PH}$ = 17.17 Hz, CHCH_3), 1.33 (3H, dd, $^3J_{HH}$ = 7.36 Hz, $^3J_{PH}$ = 17.13 Hz, CHCH_3), 1.34 (3H, dd, $^3J_{HH}$ = 7.36 Hz, $^3J_{PH}$ = 15.93 Hz, CHCH_3), 1.41 (3H, dd, $^3J_{HH}$ = 7.36 Hz, $^3J_{PH}$ = 15.97 Hz, CHCH_3), 1.58 (3H, dd, $^3J_{HH}$ = 7.32 Hz, $^3J_{PH}$ = 15.93 Hz, CHCH_3), 1.75 (3H, dd, $^3J_{HH}$ = 7.36 Hz, $^3J_{PH}$ = 17.17 Hz, CHCH_3), 2.74 (2H, pseudo quin, $^3J_{HH}$ = 7.36 Hz, CHCH$_3$), 3.02 (3H, s, OCH_3), 3.16 (3H, s, OCH_3), 3.21−3.30 (2H, m, CHCH$_3$), 5.94 (dd, 1H, $^3J_{HH}$ = 8.60 Hz, $^4J_{HH}$ = 2.44 Hz, H$_{arom}$), 6.36 (dd, 1H, $^3J_{HH}$ = 8.60 Hz, $^4J_{HH}$ = 2.48 Hz, H$_{arom}$), 6.61 (d, 1H, $^4J_{HH}$ = 2.48 Hz, H$_{arom}$), 6.66 (d, 1H, $^4J_{HH}$ = 2.44 Hz, H$_{arom}$), 7.28 (d, 1H, $^3J_{HH}$ = 8.60 Hz, H$_{arom}$), 7.50 (d, 1H, $^3J_{HH}$ = 8.60 Hz, H$_{arom}$). ^{13}C{^{1}H} NMR (C_6D_6, ppm): 14.09 (d, $^2J_{CP}$ = 6.15 Hz,

$CHCH_3$), 14.30 (d, $^2J_{CP}$ = 1.92 Hz, $CHCH_3$), 14.88 (d, $^2J_{CP}$ = 3.84 Hz, $CHCH_3$), 15.27 (s, $CHCH_3$), 16.50 (d, $^2J_{CP}$ = 4.99 Hz, $CHCH_3$), 16.80 (d, $^2J_{CP}$ = 2.69 Hz, $CHCH_3$), 17.39 (d, $^2J_{CP}$ = 5.38 Hz, $CHCH_3$), 17.84 (s, $CHCH_3$), 29.02 (dd, $^1J_{CP}$ = 21.91 Hz, $^3J_{CP}$ = 6.15 Hz, $CHCH_3$), 29.54 (d, $^1J_{CP}$ = 22.68 Hz, $CHCH_3$), 29.73 (dd, $^1J_{CP}$ = 14.99 Hz, $^3J_{CP}$ = 5.00 Hz, $CHCH_3$), 30.14 (dd, $^1J_{CP}$ = 18.45 Hz, $^3J_{CP}$ = 5.38 Hz, $CHCH_3$), 54.20 (s, OCH_3), 54.60 (s, OCH_3), 99.26 (d, $^3J_{CP}$ = 13.84 Hz, CH_{arom}, DEPT), 105.13 (d, $^3J_{CP}$ = 6.15 Hz, CH_{arom}, DEPT), 108.10 (s, CH_{arom}, DEPT), 108.31 (s, CH_{arom}, DEPT), 117.31 (dd, $^3J_{CP}$ = 18.83 Hz, $^2J_{RhC}$ = 3.46 Hz, C_{arom}), 122.37 (ddd, $^1J_{RhC}$ = 40.36 Hz, $^2J_{CPcis}$ = 6.53 Hz, $^2J_{CPcis}$ = 3.46 Hz, RhC_{Aryl}), 130.82 (s, CH_{arom}, DEPT), 141.32 (d, $^3J_{CP}$ = 5.38 Hz, CH_{arom}, DEPT), 155.96 (d, $^2J_{CP}$ = 1.92 Hz, COP), 157.52 (s, $C_{arom}OCH_3$), 161.93 (s, $C_{arom}OCH_3$), 166.78 (dd, $^2J_{CP}$ = 2.69 Hz, $^3J_{CP}$ = 15.76 Hz, COP), 198.05 (ddd, $^1J_{RhC}$ = 28.83 Hz, $^2J_{CPcis}$ = 11.92 Hz, $^2J_{CPcis}$ = 3.84 Hz, $RhCO_{Acyl}$). $^{31}P\{^1H\}$ NMR (C_7D_8, ppm): 154.89 (dd, $^2J_{PP}$ = 400.96 Hz, $^1J_{RhP}$ = 133.66 Hz), 176.31 (dd, $^2J_{PP}$ = 400.96 Hz, $^1J_{RhP}$ = 130.68 Hz). IR (ATR) [cm^{-1}]: 1603 (CO_{Acyl}). MS (FAB, *m/z*): 644 [M] (41%) with correct isotopic pattern for $C_{27}H_{40}ClO_5P_2Rh$, 616 [M − CO] (86%) with correct isotopic pattern for $C_{26}H_{40}ClO_4P_2Rh$, 609 [M − Cl] (100%) with correct isotopic pattern for $C_{27}H_{40}O_5P_2Rh$. Anal. Calcd for $C_{27}H_{40}ClO_5P_2Rh$: C: 50.28, H: 6.25. Found: C: 50.41, H: 6.08.

(2,2′-(Ethene-1,1-diyl)bis(2,1-phenylene))bis(oxy)bis-(diisopropylphosphine). The ligand synthesis was done in four steps starting from 2,2′-dihydroxybenzophenone according to known literature procedures.[7,17,18]

^1H NMR ($CDCl_3$, ppm): 0.81 (12H, dd, $^3J_{HH}$ = 7.32 Hz, $^3J_{PH}$ = 11.00 Hz, $CHCH_3$), 0.92 (12H, dd, $^3J_{HH}$ = 7.32 Hz, $^3J_{PH}$ = 15.93 Hz, $CHCH_3$), 1.60 (4H, pseudo t, $^3J_{HH}$ = 7.35 Hz, $CHCH_3$), 5.45 (2H, s, CCH_2), 6.88 (2H, pseudo t, $^3J_{HH}$ = 7.36 Hz, H_{arom}), 7.13 (2H, pseudo t, $^3J_{HH}$ = 7.36 Hz, H_{arom}), 7.23 (4H, pseudo d, $^3J_{HH}$ = 4.92 Hz, H_{arom}). $^{13}C\{^1H\}$ NMR ($CDCl_3$, ppm): 16.92 (d, $^2J_{CP}$ = 7.99 Hz, $CHCH_3$), 17.54 (d, $^2J_{CP}$ = 20.78 Hz, $CHCH_3$), 27.73 (d, $^1J_{CP}$ = 17.58 Hz, $CHCH_3$), 116.26 (d, $^3J_{CP}$ = 22.37 Hz, CH_{arom}, DEPT), 118.73 (s, $C_{Olefin}H_2$, DEPT), 120.70 (s, CH_{arom}, DEPT), 127.99 (s, CH_{arom}, DEPT), 130.68 (s, CH_{arom}, DEPT), 133.07 (s, C_{arom}), 146.62 (s, C_{Olefin}), 156.09 (d, $^2J_{CP}$ = 7.99 Hz, COP). $^{31}P\{^1H\}$ NMR ($CDCl_3$, ppm): 138.15 (s).

Synthesis of 2′. The same reaction conditions and purification procedure as described for **2** was used for **2′**. A bright yellow powder is obtained (yield: 65%) after lyophilization from benzene.

***trans*-κ^2-*P*,*P*-Rh(Cl)η^2-CH_2=C((C_6H_4)-*o*-O-P($^iC_3H_7$)$_2$)$_2$ (2′).** ^1H NMR (C_6D_6, ppm): 0.95 (3H, dd, $^3J_{HH}$ = 6.12 Hz, $^3J_{PH}$ = 14.72 Hz, $CHCH_3$), 1.03 (3H, dd, $^3J_{HH}$ = 6.12 Hz, $^3J_{PH}$ = 11.04 Hz, $CHCH_3$), 1.07 (3H, dd, $^3J_{HH}$ = 7.36 Hz, $^3J_{PH}$ = 15.93 Hz, $CHCH_3$), 1.21 (3H, dd, $^3J_{HH}$ = 7.36 Hz, $^3J_{PH}$ = 18.41 Hz, $CHCH_3$), 1.23 (3H, dd, $^3J_{HH}$ = 7.32 Hz, $^3J_{PH}$ = 15.93 Hz, $CHCH_3$), 1.44 (3H, dd, $^3J_{HH}$ = 7.32 Hz, $^3J_{PH}$ = 15.93 Hz, $CHCH_3$), 1.48 (3H, dd, $^3J_{HH}$ = 7.32 Hz, $^3J_{PH}$ = 12.24 Hz, $CHCH_3$), 1.57 (3H, dd, $^3J_{HH}$ = 7.32 Hz, $^3J_{PH}$ = 17.13 Hz, $CHCH_3$), 2.17 (dsept, 1H, $^3J_{HH}$ = 7.36 Hz, $^2J_{PH}$ = 4.92 Hz, $CHCH_3$), 2.41 (dsept, 1H, $^3J_{HH}$ = 7.36 Hz, $^2J_{PH}$ = 3.68 Hz, $CHCH_3$), 2.59 (pseudo sept, 1H, $^3J_{HH}$ = 7.36 Hz, $CHCH_3$), 2.77 (d, 1H, $^3J_{PH}$ = 3.68, CCH_2), 2.96 (pseudo dquin, 2H, $^3J_{HH}$ = 7.36 Hz, $^2J_{PH}$ = 2.44 Hz, $CHCH_3$), 4.11 (d, 1H, $^3J_{PH}$ = 11.04, CCH_2), 6.60 (pseudo quin, 1H, $^3J_{HH}$ = 7.36 Hz, $^4J_{HH}$ = 3.64, H_{arom}), 6.67 (pseudo quin, 1H, $^3J_{HH}$ = 7.36 Hz, $^4J_{HH}$ = 3.64, H_{arom}), 6.77 (d, 2H, $^4J_{HH}$ = 4.88 Hz, H_{arom}), 6.93 (d, 2H, $^4J_{HH}$ = 3.68 Hz, H_{arom}), 7.03 (d, 1H, $^3J_{HH}$ = 8.56 Hz, H_{arom}), 7.11 (d, 1H, $^3J_{HH}$ = 7.36 Hz, H_{arom}). $^{13}C\{^1H\}$ NMR (C_6D_6, ppm): 15.98 (d, $^2J_{CP}$ = 3.45 Hz, $CHCH_3$), 16.42 (d, $^2J_{CP}$ = 4.31 Hz, $CHCH_3$), 17.72 (d, $^2J_{CP}$ = 6.90 Hz, $CHCH_3$), 18.21 (d, $^2J_{CP}$ = 3.45 Hz, $CHCH_3$), 18.51 (d, $^2J_{CP}$ = 6.89 Hz, $CHCH_3$), 18.73 (s, $CHCH_3$), 19.33 (d, $^2J_{CP}$ = 3.45 Hz, $CHCH_3$), 19.43 (d, $^2J_{CP}$ = 3.45 Hz, $CHCH_3$), 28.06 (dd, $^1J_{CP}$ = 25.87 Hz, $^3J_{CP}$ = 3.45 Hz, $CHCH_3$), 29.68 (dd, $^1J_{CP}$ = 24.14 Hz, $^3J_{CP}$ = 6.04 Hz, $CHCH_3$), 29.78 (d, $^1J_{CP}$ = 14.01, $CHCH_3$), 31.12 (ddd, $^1J_{CP}$ = 11.20 Hz, $^3J_{CP}$ = 5.17 Hz, $^2J_{RhC}$ = 1.73 Hz, $CHCH_3$), 44.69 (dd, $^1J_{RhC}$ = 15.52 Hz, $^2J_{PC}$ = 6.04 Hz, C_{Olefin}), 59.61 (dd, $^1J_{RhC}$ = 13.79 Hz, $^2J_{PC}$ = 5.17 Hz, C_{Olefin}), 120.71 (d, *J* = 4.32, CH_{arom}, DEPT), 122.27 (s, CH_{arom}, DEPT), 123.15 (d, *J* = 2.59, CH_{arom}, DEPT), 124.21 (s, CH_{arom}, DEPT), 125.40 (s, CH_{arom}, DEPT), 127.87 (s, CH_{arom}, DEPT), 130.29 (d, *J* = 9.48 Hz, C_{arom}), 131.11 (s, CH_{arom}, DEPT), 136.11 (s, CH_{arom}, DEPT), 138.29 (dd, $^3J_{PC}$ = 5.17 Hz, $^2J_{RhC}$ = 2.59 Hz, C_{arom}), 152.38 (d, $^2J_{CP}$ = 2.59 Hz, COP), 153.59 (s, COP). $^{31}P\{^1H\}$ NMR (C_7D_8, ppm): 156.33 (dd, $^2J_{PP}$ = 442.53 Hz, $^1J_{RhP}$ = 136.63 Hz), 178.74 (dd, $^2J_{PP}$ = 442.53 Hz, $^1J_{RhP}$ = 133.66 Hz). MS (FAB, *m/z*): 582 [M] (90%) with correct isotopic pattern for $C_{26}H_{38}ClO_2P_2Rh$, 547 [M − Cl] (35%) with correct isotopic pattern for $C_{26}H_{38}O_2P_2Rh$. Anal. Calcd for $C_{26}H_{38}ClO_2P_2Rh$: C: 53.57, H: 6.57. Found: C: 53.03, H: 6.11.

■ ASSOCIATED CONTENT

Supporting Information. This material is available free of charge via the Internet at http://pubs.acs.org.

■ ACKNOWLEDGMENT

We thank Dr. Stephan Hoffmann for his support with the X-ray analysis.

■ REFERENCES

(1) (a) Rybtchinski, B.; Milstein, D. *Angew. Chem., Int. Ed.* **1999**, *38*, 870. (b) Chul-Ho, J. *Chem. Soc. Rev.* **2004**, *33*, 610.

(2) (a) Tipper, C. F. H. *J. Chem. Soc.* **1955**, 2045. (b) Shaltout, R. M.; Sygula, R.; Sygula, A.; Fronczek, F. R.; Stanley, G. G.; Rabideau, P. W. *J. Am. Chem. Soc.* **1998**, *120*, 835. (c) Zhang, X.; Carpenter, G. B.; Sweigart, D. A. *Organometallics* **1999**, *18*, 4887. (d) Nishimura, T.; Ohe, K.; Uemura, S. *J. Org. Chem.* **2001**, *66*, 1455. (e) Müller, C.; Lachicotte, R.; Jones, W. D. *Organometallics* **2002**, *21*, 1975. (f) Bart, S. C.; Chirik, P. J. *J. Am. Chem. Soc.* **2003**, *125*, 886.

(3) (a) Eilbracht, P.; Dahler, P. *J. Organomet. Chem.* **1977**, *135*, C23. (b) Eilbracht, P. *Chem. Ber.* **1980**, *113*, 542.(c) Benfield, F. W. S.; Green, M. L. H. *J. Chem. Soc., Dalton Trans.* **1974**, *1324*. (d) Crabtree, R. H.; Dion, R. P. *J. Chem. Soc., Chem. Commun.* **1984**, *1260*; (e) Crabtree, R. H.; Dion, R. P.; Gibboni, D. J.; McGrath, D. V.; Holt, E. M. *J. Am. Chem. Soc.* **1986**, *108*, 7222. (f) Kang, J. W.; Moseley, K.; Maitlis, P. M. *J. Am. Chem. Soc.* **1969**, *91*, 5970.(g) Dietl, H.; Maitlis, P. M. *J. Chem. Soc., Chem. Commun.* **1967**, *759*.

(4) (a) Gozin, M.; Weisman, A.; Ben-David, Y.; Milstein, D. *Nature* **1993**, *364*, 699. (b) Gozin, M.; Aizenberg, M.; Liou, S.-Y.; Weisman, A.; Ben-David, Y.; Milstein, D. *Nature* **1994**, *370*, 42.(c) Liou, S.-Y.; van der Boom, M. E.; Milstein, D. *Chem. Commun.* **1998**, 687. (d) Hartwig, J. F.; Andersen, R. A.; Bergman, R. G. *J. Am. Chem. Soc.* **1989**, *111*, 2717. (e) Kaplan, A. W.; Bergman, R. G. *Organometallics* **1997**, *16*, 1106. (f) Murakami, M.; Amii, H.; Ito, Y. *Nature* **1994**, *370*, 540. (g) Murakami, M.; Amii, H.; Shigeto, K.; Ito, Y. *J. Am. Chem. Soc.* **1996**, *118*, 8285. (h) Daugulis, O.; Brookhart, M. *Organometallics* **2004**, *23*, 527. (i) Perthuisot, C.; Jones, W. D. *J. Am. Chem. Soc.* **1994**, *116*, 3647. (j) Perthuisot, C.; Edelbach, B. L.; Zubris, D. L.; Jones, W. D. *Organometallics* **1997**, *16*, 2016. (k) Chantani, N.; Ie, Y.; Kakiuchi, F.; Murai, S. *J. Am. Chem. Soc.* **1999**, *121*, 8645. (l) Suggs, J. W.; Cox, S. D. *J. Organomet. Chem.* **1981**, *221*, 199. (m) Suggs, J. W.; Jun, C.-H. *J. Am. Chem. Soc.* **1984**, *106*, 3054. (n) Suggs, J. W.; Jun, C.-H. *J. Chem. Soc., Chem. Commun.* **1985**, 92. (o) Suggs, J. W.; Wovkulich, M. J.; Cox, S. D. *Organometallics* **1985**, *4*, 1101. (p) Suggs, J. W.; Jun, C.-H. *J. Am. Chem. Soc.* **1986**, *108*, 4679. (q) Jun, C.-H.; Lee, H. *J. Am. Chem. Soc.* **1999**, *121*, 880. (r) Jun, C.-H.; Lee, H.; Lim, S.-G. *J. Am. Chem. Soc.* **2001**, *123*, 751. (s) Dreis, A. M.; Douglas, C. J. *J. Am. Chem. Soc.* **2009**, *131*, 412. (t) Rathbun, C., M.; Johnson, J. B. *J. Am. Chem. Soc.* **2011**, *133*, 2031. (u) Wentzel, M. T.; Reddy, V. J.; Hyster, T. K.; Douglas, C. J. *Angew. Chem., Int. Ed.* **2009**, *48*, 6121.

(5) (a) Liou, S.-Y.; Gozin, M.; Milstein, D. *J. Am. Chem. Soc.* **1995**, *117*, 9774. (b) Rybtchinski, B.; Vigalok, A.; Ben-David, Y.; Milstein, D. *J. Am. Chem. Soc.* **1996**, *118*, 12406. (c) Gandelman, M.; Vigalok, A.; Shimon, J. W. L.; Milstein, D. *Organometallics* **1997**, *16*, 3981. (d) Rybtchinski, B.; Milstein, D. *J. Am. Chem. Soc.* **1999**, *121*, 4528. (e) van der Boom, M. E.; Ben-

David, Y.; Milstein, D. *J. Am. Chem. Soc.* **1999**, *121*, 6652. (f) van der Boom, M. E.; Kraatz, H.-B.; Hassner, L.; Ben-David, Y.; Milstein, D. *Organometallics* **1999**, *18*, 3873. (g) Gandelman, M.; Vigalok, A.; Konstantinovsky, L.; Milstein, D. *J. Am. Chem. Soc.* **2000**, *122*, 9848. (h) Cohen, R.; van der Boom, M. E.; Shimon, L. J. W.; Rozenberg, H.; Milstein, D. *J. Am. Chem. Soc.* **2000**, *122*, 7723. (i) Sundermann, A.; Uzan, O.; Milstein, D.; Martin, J. M. L. *J. Am. Chem. Soc.* **2000**, *122*, 7095. (j) Rybtchinski, B.; Oevers, S.; Montag, M.; Vigalok, A.; Rozenberg, H.; Martin, J. M. L.; Milstein, D. *J. Am. Chem. Soc.* **2001**, *123*, 9064. (k) Gauvin, R. M.; Rozenberg, H.; Shimon, L. J. W.; Milstein, D. *Organometallics* **2001**, *20*, 1719. (l) Gandelman, M.; Shimon, L. J. W.; Milstein, D. *Chem.—Eur. J.* **2003**, *9*, 4295. (m) van der Boom, M. E.; Liou, S.-Y.; Shimon, L. J. W.; Ben-David, Y.; Milstein, D. *Inorg. Chim. Acta* **2004**, *357*, 4015. (n) Cohen, R.; Milstein, D.; Martin, J. M. L. *Organometallics* **2004**, *23*, 2336. (o) Salem, H.; Ben-David, Y.; Shimon, L. J. W.; Milstein, D. *Organometallics* **2006**, *25*, 2292. (p) Gauvin, R. M.; Rozenberg, H.; Shimon, L. J. W.; Ben-David, Y.; Milstein, D. *Chem.—Eur. J.* **2007**, *13*, 1382.

(6) Gordon, A. J.; Ford, R. A. *The Chemist's Companion*; Wiley: New York, 1972; p 113. The C−C bond dissociation energy of ethane is 88 kcal/mol, while that for acetone is 82 kcal/mol.

(7) Ruhland, K.; Obenhuber, A.; Hoffmann, S. D. *Organometallics* **2008**, *27*, 3482.

(8) Obenhuber, A.; Ruhland, K. *Organometallics* **2011**, *30*, 171.

(9) Complete line shape analysis was done using WinDNMR Version 7.1.11, which is available from http://www.chem.wisc.edu/areas/reich/plt/windnmr.htm.

(10) **2′** is stable upon heating in toluene at 95 °C over 24 h. Slow decomposition is observed on heating **2′** in nitromethane at 100 °C after 72 h. No reaction is observed with H_2 (1 atm, rt) or H_2SiPh_2 at 95 °C over several hours. Treatment with 1.1 equiv of $AgBF_4$ in $CDCl_3$ or nitromethane at room temperature caused decomposition.

(11) (a) Baird, M. C.; Mague, J. T.; Osborn, J. A.; Wilkinson, G. *J. Chem. Soc. A* **1967**, 1347. (b) Schwartz, J.; Hart, D. W.; Holden, J. L. *J. Am. Chem. Soc.* **1972**, *94*, 9269. (c) Hegedus, L. S.; Lo, S. M.; Bloss, D. E. *J. Am. Chem. Soc.* **1973**, *95*, 3040. (d) Lau, K. S. Y.; Becker, Y.; Huang, F.; Baenziger, N.; Stille, J. K. *J. Am. Chem. Soc.* **1977**, *99*, 5664.

(12) Van der Ent, A.; Onderdelinden, A. L.; Schunn, R. A. *Inorg. Synth.* **1990**, *28*, 90.

(13) Evans, D.; Osborn, J. A.; Wilkinson, G. *Inorg. Synth.* **1967**, *10*, 79.

(14) McCleverty, J. A.; Wilkinson, G. *Inorg. Synth.* **1974**, *15*, 84.

(15) Sheldrick, G. M. *SHELXS-97, Program for the Solution of Crystal Structures*; Universität Göttingen: Göttingen, Germany, 1997. *SHELXL-97, Program for the Refinement of Crystal Structures*; Universität Göttingen: Göttingen, Germany, 1997.

(16) Frisch, M. J.; *Gaussian 03*, Revision B.01; Gaussian, Inc.: Pittsburgh, PA, 2003.

(17) Kiddle, J. J. *Tetrahedron Lett.* **2000**, *41*, 1339.

(18) Nicolaou, K. C.; Snyder, S. A.; Huang, X.; Simonsen, K. B.; Koumbis, A. E.; Bigot, A. J. *J. Am. Chem. Soc.* **2004**, *126*, 10162.